

1 **Radio-Loud Narrow-Line Seyfert 1**  
2 **as a New Class of Gamma-Ray AGN**

3 A. A. Abdo<sup>1,2</sup>, M. Ackermann<sup>3</sup>, M. Ajello<sup>3</sup>, L. Baldini<sup>4</sup>, J. Ballet<sup>5</sup>, G. Barbiellini<sup>6,7</sup>,  
4 D. Bastieri<sup>8,9</sup>, K. Bechtol<sup>3</sup>, R. Bellazzini<sup>4</sup>, B. Berenji<sup>3</sup>, E. D. Bloom<sup>3</sup>, E. Bonamente<sup>10,11</sup>,  
5 A. W. Borgland<sup>3</sup>, J. Bregeon<sup>4</sup>, A. Brez<sup>4</sup>, M. Brigida<sup>12,13</sup>, P. Bruel<sup>14</sup>, T. H. Burnett<sup>15</sup>,  
6 G. A. Caliandro<sup>16</sup>, R. A. Cameron<sup>3</sup>, P. A. Caraveo<sup>17</sup>, J. M. Casandjian<sup>5</sup>, C. Cecchi<sup>10,11</sup>,  
7 Ö. Çelik<sup>18,19,20</sup>, A. Chekhtman<sup>1,21</sup>, C. C. Cheung<sup>1,2</sup>, J. Chiang<sup>3</sup>, S. Ciprini<sup>11</sup>, R. Claus<sup>3</sup>,  
8 J. Cohen-Tanugi<sup>22</sup>, J. Conrad<sup>23,24,25</sup>, S. Cutini<sup>26</sup>, C. D. Dermer<sup>1</sup>, F. de Palma<sup>12,13</sup>,  
9 E. do Couto e Silva<sup>3</sup>, P. S. Drell<sup>3</sup>, R. Dubois<sup>3</sup>, D. Dumora<sup>27,28</sup>, C. Farnier<sup>22</sup>, C. Favuzzi<sup>12,13</sup>,  
10 S. J. Fegan<sup>14</sup>, W. B. Focke<sup>3</sup>, L. Foschini<sup>29,58</sup>, M. Frailis<sup>31</sup>, Y. Fukazawa<sup>32</sup>, P. Fusco<sup>12,13</sup>,  
11 F. Gargano<sup>13</sup>, N. Gehrels<sup>18,33,34</sup>, S. Germani<sup>10,11</sup>, B. Giebels<sup>14</sup>, N. Giglietto<sup>12,13</sup>,  
12 F. Giordano<sup>12,13</sup>, M. Giroletti<sup>35</sup>, T. Glanzman<sup>3</sup>, G. Godfrey<sup>3</sup>, I. A. Grenier<sup>5</sup>, J. E. Grove<sup>1</sup>,  
13 L. Guillemot<sup>36</sup>, S. Guiriec<sup>37</sup>, M. Hayashida<sup>3</sup>, E. Hays<sup>18</sup>, D. Horan<sup>14</sup>, R. E. Hughes<sup>38</sup>,  
14 G. Jóhannesson<sup>3</sup>, A. S. Johnson<sup>3</sup>, W. N. Johnson<sup>1</sup>, M. Kadler<sup>39,19,40,41</sup>, T. Kamae<sup>3</sup>,  
15 H. Katagiri<sup>32</sup>, J. Kataoka<sup>42</sup>, M. Kerr<sup>15</sup>, J. Knödseder<sup>43</sup>, M. Kuss<sup>4</sup>, J. Lande<sup>3</sup>,  
16 L. Latronico<sup>4</sup>, F. Longo<sup>6,7</sup>, F. Loparco<sup>12,13</sup>, B. Lott<sup>27,28</sup>, M. N. Lovellette<sup>1</sup>, P. Lubrano<sup>10,11</sup>,  
17 A. Makeev<sup>1,21</sup>, M. N. Mazziotta<sup>13</sup>, W. McConville<sup>18,34</sup>, J. E. McEnery<sup>18,34</sup>, C. Meurer<sup>23,24</sup>,  
18 P. F. Michelson<sup>3</sup>, W. Mitthumsiri<sup>3</sup>, T. Mizuno<sup>32</sup>, C. Monte<sup>12,13</sup>, M. E. Monzani<sup>3</sup>,  
19 A. Morselli<sup>44</sup>, I. V. Moskalenko<sup>3</sup>, S. Murgia<sup>3</sup>, P. L. Nolan<sup>3</sup>, J. P. Norris<sup>45</sup>, E. Nuss<sup>22</sup>,  
20 T. Ohsugi<sup>32</sup>, N. Omodei<sup>4</sup>, E. Orlando<sup>46</sup>, J. F. Ormes<sup>45</sup>, V. Pelassa<sup>22</sup>, M. Pepe<sup>10,11</sup>,  
21 M. Persic<sup>47,6</sup>, M. Pesce-Rollins<sup>4</sup>, F. Piron<sup>22</sup>, T. A. Porter<sup>48</sup>, S. Rainò<sup>12,13</sup>, R. Rando<sup>8,9</sup>,  
22 M. Razzano<sup>4</sup>, L. S. Rochester<sup>3</sup>, A. Y. Rodriguez<sup>16</sup>, F. Ryde<sup>49,24</sup>, H. F.-W. Sadrozinski<sup>48</sup>,  
23 R. Sambruna<sup>18</sup>, A. Sander<sup>38</sup>, P. M. Saz Parkinson<sup>48</sup>, J. D. Scargle<sup>50</sup>, C. Sgrò<sup>4</sup>,  
24 P. D. Smith<sup>38</sup>, G. Spandre<sup>4</sup>, P. Spinelli<sup>12,13</sup>, M. S. Strickman<sup>1</sup>, D. J. Suson<sup>51</sup>,  
25 G. Tagliaferri<sup>29</sup>, H. Takahashi<sup>32</sup>, T. Takahashi<sup>52</sup>, T. Tanaka<sup>3</sup>, J. B. Thayer<sup>3</sup>, J. G. Thayer<sup>3</sup>,  
26 D. J. Thompson<sup>18</sup>, L. Tibaldo<sup>8,9,5</sup>, O. Tibolla<sup>53</sup>, D. F. Torres<sup>54,16</sup>, G. Tosti<sup>10,11</sup>,  
27 A. Tramacere<sup>3,55</sup>, Y. Uchiyama<sup>3</sup>, T. L. Usher<sup>3</sup>, V. Vasileiou<sup>19,20</sup>, N. Vilchez<sup>43</sup>, V. Vitale<sup>44,56</sup>,  
28 A. P. Waite<sup>3</sup>, P. Wang<sup>3</sup>, B. L. Winer<sup>38</sup>, K. S. Wood<sup>1</sup>, T. Ylinen<sup>49,57,24</sup>, M. Ziegler<sup>48</sup> (The  
29 *Fermi*/LAT Collaboration)

30 and

31 G. Ghisellini<sup>29</sup>, L. Maraschi<sup>29</sup>, F. Tavecchio<sup>29</sup>

---

<sup>1</sup>Space Science Division, Naval Research Laboratory, Washington, DC 20375, USA

<sup>2</sup>National Research Council Research Associate, National Academy of Sciences, Washington, DC 20001, USA

<sup>3</sup>W. W. Hansen Experimental Physics Laboratory, Kavli Institute for Particle Astrophysics and Cosmology, Department of Physics and SLAC National Accelerator Laboratory, Stanford University, Stanford, CA 94305, USA

<sup>4</sup>Istituto Nazionale di Fisica Nucleare, Sezione di Pisa, I-56127 Pisa, Italy

<sup>5</sup>Laboratoire AIM, CEA-IRFU/CNRS/Université Paris Diderot, Service d’Astrophysique, CEA Saclay, 91191 Gif sur Yvette, France

<sup>6</sup>Istituto Nazionale di Fisica Nucleare, Sezione di Trieste, I-34127 Trieste, Italy

<sup>7</sup>Dipartimento di Fisica, Università di Trieste, I-34127 Trieste, Italy

<sup>8</sup>Istituto Nazionale di Fisica Nucleare, Sezione di Padova, I-35131 Padova, Italy

<sup>9</sup>Dipartimento di Fisica “G. Galilei”, Università di Padova, I-35131 Padova, Italy

<sup>10</sup>Istituto Nazionale di Fisica Nucleare, Sezione di Perugia, I-06123 Perugia, Italy

<sup>11</sup>Dipartimento di Fisica, Università degli Studi di Perugia, I-06123 Perugia, Italy

<sup>12</sup>Dipartimento di Fisica “M. Merlin” dell’Università e del Politecnico di Bari, I-70126 Bari, Italy

<sup>13</sup>Istituto Nazionale di Fisica Nucleare, Sezione di Bari, 70126 Bari, Italy

<sup>14</sup>Laboratoire Leprince-Ringuet, École polytechnique, CNRS/IN2P3, Palaiseau, France

<sup>15</sup>Department of Physics, University of Washington, Seattle, WA 98195-1560, USA

<sup>16</sup>Institut de Ciències de l’Espai (IEEC-CSIC), Campus UAB, 08193 Barcelona, Spain

<sup>17</sup>INAF Istituto di Astrofisica Spaziale e Fisica Cosmica, I-20133 Milano, Italy

<sup>18</sup>NASA Goddard Space Flight Center, Greenbelt, MD 20771, USA

<sup>19</sup>Center for Research and Exploration in Space Science and Technology (CRESST) and NASA Goddard Space Flight Center, Greenbelt, MD 20771, USA

<sup>20</sup>Department of Physics and Center for Space Sciences and Technology, University of Maryland Baltimore County, Baltimore, MD 21250, USA

<sup>21</sup>George Mason University, Fairfax, VA 22030, USA

<sup>22</sup>Laboratoire de Physique Théorique et Astroparticules, Université Montpellier 2, CNRS/IN2P3, Montpellier, France

<sup>23</sup>Department of Physics, Stockholm University, AlbaNova, SE-106 91 Stockholm, Sweden

<sup>24</sup>The Oskar Klein Centre for Cosmoparticle Physics, AlbaNova, SE-106 91 Stockholm, Sweden

<sup>25</sup>Royal Swedish Academy of Sciences Research Fellow, funded by a grant from the K. A. Wallenberg

---

Foundation

<sup>26</sup>Agenzia Spaziale Italiana (ASI) Science Data Center, I-00044 Frascati (Roma), Italy

<sup>27</sup>Université de Bordeaux, Centre d'Études Nucléaires Bordeaux Gradignan, UMR 5797, Gradignan, 33175, France

<sup>28</sup>CNRS/IN2P3, Centre d'Études Nucléaires Bordeaux Gradignan, UMR 5797, Gradignan, 33175, France

<sup>29</sup>INAF Osservatorio Astronomico di Brera, I-23807 Merate, Italy; [luigi.foschini@brera.inaf.it](mailto:luigi.foschini@brera.inaf.it)

<sup>30</sup>Corresponding author: L. Foschini, [luigi.foschini@brera.inaf.it](mailto:luigi.foschini@brera.inaf.it).

<sup>31</sup>Dipartimento di Fisica, Università di Udine and Istituto Nazionale di Fisica Nucleare, Sezione di Trieste, Gruppo Collegato di Udine, I-33100 Udine, Italy

<sup>32</sup>Department of Physical Sciences, Hiroshima University, Higashi-Hiroshima, Hiroshima 739-8526, Japan

<sup>33</sup>Department of Astronomy and Astrophysics, Pennsylvania State University, University Park, PA 16802, USA

<sup>34</sup>Department of Physics and Department of Astronomy, University of Maryland, College Park, MD 20742, USA

<sup>35</sup>INAF Istituto di Radioastronomia, 40129 Bologna, Italy

<sup>36</sup>Max-Planck-Institut für Radioastronomie, Auf dem Hügel 69, 53121 Bonn, Germany

<sup>37</sup>Center for Space Plasma and Aeronomic Research (CSPAR), University of Alabama in Huntsville, Huntsville, AL 35899, USA

<sup>38</sup>Department of Physics, Center for Cosmology and Astro-Particle Physics, The Ohio State University, Columbus, OH 43210, USA

<sup>39</sup>Dr. Remeis-Sternwarte Bamberg, Sternwartstrasse 7, D-96049 Bamberg, Germany

<sup>40</sup>Erlangen Centre for Astroparticle Physics, D-91058 Erlangen, Germany

<sup>41</sup>Universities Space Research Association (USRA), Columbia, MD 21044, USA

<sup>42</sup>Waseda University, 1-104 Totsukamachi, Shinjuku-ku, Tokyo, 169-8050, Japan

<sup>43</sup>Centre d'Étude Spatiale des Rayonnements, CNRS/UPS, BP 44346, F-30128 Toulouse Cedex 4, France

<sup>44</sup>Istituto Nazionale di Fisica Nucleare, Sezione di Roma “Tor Vergata”, I-00133 Roma, Italy

<sup>45</sup>Department of Physics and Astronomy, University of Denver, Denver, CO 80208, USA

<sup>46</sup>Max-Planck Institut für extraterrestrische Physik, 85748 Garching, Germany

<sup>47</sup>Osservatorio Astronomico di Trieste, Istituto Nazionale di Astrofisica, I-34143 Trieste, Italy

<sup>48</sup>Santa Cruz Institute for Particle Physics, Department of Physics and Department of Astronomy and Astrophysics, University of California at Santa Cruz, Santa Cruz, CA 95064, USA

<sup>49</sup>Department of Physics, Royal Institute of Technology (KTH), AlbaNova, SE-106 91 Stockholm, Sweden

## ABSTRACT

We report the discovery with *Fermi*/LAT of  $\gamma$ -ray emission from three radio-loud narrow-line Seyfert 1 galaxies: PKS 1502+036 ( $z = 0.409$ ), 1H 0323+342 ( $z = 0.061$ ) and PKS 2004-447 ( $z = 0.24$ ). In addition to PMN J0948+0022 ( $z = 0.585$ ), the first source of this type to be detected in  $\gamma$  rays, they may form an emerging new class of  $\gamma$ -ray active galactic nuclei (AGN). These findings can have strong implications on our knowledge about relativistic jets and the unified model of AGN.

*Subject headings:* quasars: general – galaxies: active – galaxies: Seyfert – gamma rays: observations

## 1. Introduction

The advent of the *Fermi Gamma-ray Space Telescope* (hereafter, *Fermi*), with its excellent performance, is changing our perception of the sky at high-energy  $\gamma$  rays. Specifically, the recent detection in the MeV-GeV energy range of the radio-loud narrow-line Seyfert 1 (RL-NLS1) quasar PMN J0948+0022 strongly supports the presence of a closely aligned relativistic jet in this peculiar system (Abdo et al. 2009a,c; Foschini et al. 2009a). This is quite surprising, since NLS1s are generally hosted in spiral galaxies and the presence of a fully developed relativistic jet is contrary to the well-known paradigm that this type of system is associated to ellipticals (e.g. see Marscher 2009 for a recent review).

---

<sup>50</sup>Space Sciences Division, NASA Ames Research Center, Moffett Field, CA 94035-1000, USA

<sup>51</sup>Department of Chemistry and Physics, Purdue University Calumet, Hammond, IN 46323-2094, USA

<sup>52</sup>Institute of Space and Astronautical Science, JAXA, 3-1-1 Yoshinodai, Sagamihara, Kanagawa 229-8510, Japan

<sup>53</sup>Max-Planck-Institut für Kernphysik, D-69029 Heidelberg, Germany

<sup>54</sup>Institució Catalana de Recerca i Estudis Avançats (ICREA), Barcelona, Spain

<sup>55</sup>Consorzio Interuniversitario per la Fisica Spaziale (CIFS), I-10133 Torino, Italy

<sup>56</sup>Dipartimento di Fisica, Università di Roma “Tor Vergata”, I-00133 Roma, Italy

<sup>57</sup>School of Pure and Applied Natural Sciences, University of Kalmar, SE-391 82 Kalmar, Sweden

<sup>58</sup>Author to whom any correspondence should be addressed.

45 Already in the past, several authors inferred from the multiwavelength properties of  
 46 RL-NLS1s some parallelism between this type of source and blazars (e.g. Komossa et al.  
 47 2006, Yuan et al. 2008, Foschini et al. 2009b), suggesting similarities with different flavors  
 48 of the blazar types (quasars or BL Lacs). What was missing in these previous studies is the  
 49  $\gamma$ -ray detection, which is important to confirm the presence of a relativistic jet, to measure  
 50 its power, and to study the characteristics of this type of sources by modeling their spectral  
 51 energy distributions (SEDs). Indeed, blazar-like radio emission from radio-quiet AGNs has  
 52 been already reported (e.g., Brunthaler et al. 2000, Brunthaler et al. 2005, Lister et al.  
 53 2009; see also the review by Ho 2008), but no  $\gamma$  rays have been yet detected from these  
 54 sources. This suggests some evident differences between fully developed relativistic jets (i.e.  
 55 emitting over the whole electromagnetic spectrum, from radio to  $\gamma$  rays) and jet-like (perhaps  
 56 aborted?, cf Ghisellini et al. 2004) structures, whose emission at  $\gamma$  rays in the MeV-TeV  
 57 energy range – if any – has not been yet reported.

58 Understanding these differences could give important insights into jet formation. There-  
 59 fore, we started a larger program aiming at the detection of  $\gamma$ -ray emission from other RL-  
 60 NLS1s. Since no complete sample of RL-NLS1s is available in the literature, we have built  
 61 a sample by merging all the sources of this type in the catalog of Zhou & Wang (2002) and  
 62 in the lists of Komossa et al. (2006) and Yuan et al. (2008). We have adopted a threshold  
 63 in the radio-loudness  $R_L = f_{5\text{ GHz}}/f_{440\text{ nm}} = 50$ , in order to avoid doubtful sources at the  
 64 border ( $R_L = 10$ ) with radio-quietness. The optical properties are those typical of NLS1s,  
 65 i.e. narrow permitted lines (FWHM  $H\beta < 2000\text{ km s}^{-1}$ ),  $[OIII]/H\beta < 3$  and the bump of FeII  
 66 (see Pogge 2000 for a review). At radio frequencies, RL-NLS1s display strong and variable  
 67 radio emission, with brightness temperature well above the inverse-Compton limit (see, e.g.,  
 68 Yuan et al. 2008, Table 3).

69 This selection resulted in a list of 29 sources, most of them selected from the *Sloan Digital*  
 70 *Sky Survey* (SDSS). This low number should not be a surprise. According to Komossa et  
 71 al. (2006), RL-NLS1s are more rare than quasars: 7% of NLS1s have  $R_L > 10$  and only  
 72 2.5% exceed  $R_L = 50$ , while generally 10-20% of quasars are radio-loud. Although based  
 73 on a small sample of objects (128), these results have been confirmed by studies on larger  
 74 samples from the SDSS (Zhou et al. 2006, Whalen et al. 2006). It is worth noting that this  
 75 sample is not complete, although the fact that it is based on the SDSS ensures a minimum  
 76 degree of representativeness.

77 Here we report three new detections at  $\gamma$  rays of RL-NLS1s obtained with *Fermi*/LAT.  
 78 In addition to the already known PMN J0948+0022 (reported by Abdo et al. 2009a,c;  
 79 Foschini et al. 2009a), this increases the number of  $\gamma$ -ray detections of NLS1s (3 + 1 = 4  
 80 out of 29 sources,  $\approx 14\%$  of our sample), suggesting that they form a new class of  $\gamma$ -ray

81 emitting AGNs.

82 Throughout this work, we adopted a  $\Lambda$ CDM cosmology from the most recent *WMAP*  
 83 results, which give the following values for the cosmological parameters:  $h = 0.71$ ,  $\Omega_m = 0.27$ ,  
 84  $\Omega_\Lambda = 0.73$  and with the Hubble-Lemaître constant  $H_0 = 100h \text{ km s}^{-1} \text{ Mpc}^{-1}$  (Komatsu et  
 85 al. 2009).

## 86 2. Data Analysis

87 The data from the Large Area Telescope (LAT, Atwood et al. 2009) onboard *Fermi*  
 88 were analyzed following the same scheme described in Abdo et al. (2009a), but using a more  
 89 recent version of the software (`Science Tools v 9.15.2`), Instrument Response Function  
 90 (IRF P6\_V3\_DIFFUSE, Rando et al. 2009) and background subtraction<sup>1</sup>. The data analyzed  
 91 span between MJD 54682 (2008 August 4) and 55048 (2009 August 5).

92 Four LAT sources with  $\text{TS}^2$  greater than 25, which is equivalent<sup>3</sup> to  $\sim 5\sigma$ , can be  
 93 associated with RL-NLS1s by using the Figure-of-Merit (FoM) method outlined in Abdo  
 94 et al. (2009b) and already used to associate other LAT sources with radio counterparts.  
 95 One of them is the already well-known PMN J0948+0022 (Abdo et al. 2009a). The three  
 96 remaining new sources were associated to the RL-NLS1 objects PKS 1502+036 ( $z = 0.409$ ),  
 97 1H 0323+342 ( $z = 0.061$ ) and PKS 2004-447 ( $z = 0.24$ ). The results are summarized in  
 98 Table 1.

99 In order to build SEDs, we retrieved all the publicly available data of these sources. In  
 100 the case of PKS 1502+036, no X-ray data were found and, therefore, we asked for a 5 ks snap-  
 101 shot with the *Swift* satellite, which was performed on 2009 July 25 (ObsID 00031445001). We  
 102 retrieved from the public *Swift* archives, optical/UV/X-rays data also for PMN J0948+0022  
 103 (Abdo et al. 2009a) and 1H 0323+342. For the latter, we analyzed all the observations  
 104 performed between 2006 July 6 and 2008 November 16 (15 observations) and averaged the  
 105 results (total exposure on XRT was 57 ks). In the case of PKS 2004-447, one *XMM-Newton*  
 106 observation was found (ObsID 0200360201, performed on 2004 April 11; 42 ks exposure on  
 107 EPIC, see Gallo et al. 2006) and analyzed.

---

<sup>1</sup>We adopted the same version of software and calibration database that is publicly available at <http://fermi.gsfc.nasa.gov/ssc/data/analysis/software/>.

<sup>2</sup>Likelihood test statistic, see Mattox et al. (1996) for a definition of this test.

<sup>3</sup>The significance of the detection in  $\sigma$  is roughly  $\sqrt{\text{TS}}$ .

Table 1:  $\gamma$ -ray characteristics of RL-NLS1s detected by LAT with  $TS > 25$ .

Name	$z$	$\alpha$ [deg]	$\delta$ [deg]	$r_{95\%}^a$ [deg]	$F_\gamma^b$ [ $10^{-8}$ ph cm $^{-2}$ s $^{-1}$ ]	$\Gamma^c$	$TS$	$L_\gamma^d$ [ $10^{46}$ erg s $^{-1}$ ]	Ass. <sup>e</sup> [%]
1H 0323+342	0.061	51.27	+34.19	0.21	$5.7 \pm 0.3$	$2.74 \pm 0.03$	78	0.02	92
PKS 1502+036	0.409	226.26	+3.37	0.18	$7.5 \pm 0.3$	$2.81 \pm 0.03$	186	2.1	93
PKS 2004-447	0.24	301.99	-44.51	0.09	$2.3 \pm 0.3$	$2.5 \pm 0.4$	43	0.2	81
PMN J0948+0022 <sup>f</sup>	0.585	147.28	+0.39	0.12	$14.6 \pm 0.9$	$2.78 \pm 0.06$	647	11	99

<sup>a</sup>Error radius at 95% confidence level. To take properly into account systematic effects in the calculation of the error radii, we added the absolute systematic error of  $0^\circ.0075$  in quadrature to the 68%, then we convert to 95% by multiplying by 1.62 and, finally, we multiply by 1.2, which is the relative systematic error (Abdo et al., in preparation).

<sup>b</sup> $\gamma$ -ray flux for  $E > 100$  MeV. We quoted only statistical errors, while the systematics to be considered are 10% at 100 MeV, 5% at 500 MeV and 20% at 10 GeV (Rando et al. 2009).

<sup>c</sup>Photon index of the power-law model used to fit LAT data.

<sup>d</sup>Observed  $\gamma$ -ray luminosity.

<sup>e</sup>Confidence level of the association according to the FoM.

<sup>f</sup>See Abdo et al. (2009a).

108 PMN J0948+0022 was extensively studied in Abdo et al. (2009a,c), while the data of  
 109 1H 0323+342 and PKS 2004-447 were already discussed in Foschini et al. (2009b). Partic-  
 110 ularly, we found in the case of 1H 0323+342, there is evidence of spectral variability in the  
 111 X-ray energy band, even on timescales of a few days. The photon index is generally soft, as  
 112 for a typical NLS1 (cf Leighly 1999), but sometimes it displays a hard tail ( $\Gamma \approx 1.3 - 1.6$ )  
 113 during a simultaneous increase of the optical/UV flux (Foschini et al. 2009b).

114 PKS 1502+036 was first observed in X-rays on 2009 July 25 (*Swift* ObsID 00031445001).  
 115 No previous X-ray observations were available and even *ROSAT* measured just an upper  
 116 limit, which was not very stringent ( $< 2 \times 10^{-12}$  erg cm $^{-2}$  s $^{-1}$  in the 0.1 – 2.4 keV, see  
 117 Yuan et al. 2008). We based our plans for the observation taking into account the similar  
 118 optical characteristics shared with the better known PMN J0948+0022 (Abdo et al. 2009a).  
 119 However, the effective exposure of 4.6 ks on XRT was not long enough to collect sufficient  
 120 photons to apply the  $\chi^2$  test statistic. Therefore, we grouped the photons to have at least 10  
 121 counts per bin and applied the Cash statistic, which allows the parameters to be estimated  
 122 through the likelihood ratio (Cash 1979).

123 In order to make a homogeneous data set, we have reanalyzed all the *Swift* and *XMM-*  
 124 *Newton* data adopting the same procedures outlined in the previous works, but using the  
 125 most recent software packages version (HEASOFT v. 6.6.3 for *Swift* and SAS v. 9.0.0 for  
 126 *XMM-Newton*) and calibration databases (updated on 2009 June 5 for *Swift* and 2009 June

Table 2: Summary of the *Swift* and *XMM-Newton* analyses.

Source	Inst <sup>a</sup>	Exp <sup>b</sup>	$N_{\text{H}}^{\text{c}}$	X-rays			$F^{\text{g}}$	Stat <sup>h</sup>
				$\Gamma^{\text{d}}$	$E_{\text{b}}^{\text{e}}$	$\Gamma_2^{\text{f}}$		
1H 0323+342	X	57.1	11.7	$2.03 \pm 0.02^{\text{i}}$	–	–	$14.0 \pm 0.1$	1.06/313
PKS 1502+036	X	4.6	3.89	$1.0^{+0.9}_{-0.8}$	–	–	$0.43 \pm 0.10$	2
PKS 2004-447	E	15, 22, 22	2.96	$2.0^{+0.2}_{-0.1}$	$0.67 \pm 0.08$	$1.50 \pm 0.03$	$1.5 \pm 0.1$	1.05/315

Source	Inst <sup>a</sup>	$A_{\text{V}}^{\text{l}}$	$v$	Optical/UV			$uvw1$	$uvw2$	$uvw2$
				$b$	$u$	$u$			
1H 0323+342	U	0.62	$15.82 \pm 0.03$	$16.38 \pm 0.03$	$15.50 \pm 0.03$	$15.82 \pm 0.04$	$16.01 \pm 0.04$	$15.92 \pm 0.04$	
PKS 1502+036	U	0.21	$19.0 \pm 0.2$	$19.5 \pm 0.1$	$18.6 \pm 0.1$	$18.54 \pm 0.08$	$18.38 \pm 0.08$	$18.40 \pm 0.06$	
PKS 2004-447	O	0.16	–	$18.91 \pm 0.08$	$18.54 \pm 0.09$	$18.65 \pm 0.08$	$19.0 \pm 0.2$	–	

<sup>a</sup>Instrument used for the observation: X for XRT and U for UVOT onboard *Swift*; E for EPIC PN, MOS1, and MOS2 and O for OM onboard *XMM-Newton*.

<sup>b</sup>Net exposure in kiloseconds. In the case of EPIC, the exposures of PN, MOS1 and MOS2, respectively, are reported.

<sup>c</sup>Galactic absorption in units of  $10^{20} \text{ cm}^{-2}$  from Kablerla et al. (2005).

<sup>d</sup>Photon index of the power-law model or low-energy photon index in the case of broken power-law model.

<sup>e</sup>Break energy in the case of broken power-law model [keV].

<sup>f</sup>High-energy photon index in the case of broken power-law model.

<sup>g</sup>Observed flux in the 0.2 – 10 keV energy band in units of  $10^{-12} \text{ erg cm}^{-2} \text{ s}^{-1}$ .

<sup>h</sup>Statistical parameters:  $\tilde{\chi}^2/dof$  for  $\chi^2$  or number of PHA bins for the Cash statistic.

<sup>i</sup>It is worth noting that the addition of an unresolved gaussian emission line at  $E = 6.5 \pm 0.3 \text{ keV}$  with equivalent width  $\sim 147 \text{ eV}$  gives a  $\Delta\chi^2 = 9.3$ .

<sup>l</sup>Magnitudes absorbed by the Galactic column in the visual filter (from Kalberla et al. 2005) and used as reference to calculate the absorption in other filters by means of the Cardelli et al. (1989) extinction law.

127 11 for *XMM-Newton*). X-ray data were fitted to power-law or broken power-law models with  
 128 Galactic absorption from Kalberla et al. (2005), while optical/UV data were dereddened for  
 129 the proper values calculated according to the extinction laws by Cardelli et al. (1989). None  
 130 of the sources showed evidence of X-ray absorption in excess to the Galactic value. The X-ray  
 131 photon indexes are generally in agreement with those typical of blazars (c.f., for example,  
 132 Foschini et al. 2006; Maraschi et al. 2008). The results are summarized in Table 2. All the  
 133 results of the present reanalysis are consistent with the previous ones already reported in  
 134 Foschini et al. (2009b).

Table 3: Parameters used to model the SEDs.

Name	$R_{\text{diss}}^a$	$\log M^b$	$R_{\text{BLR}}^c$	$P_1^d$	$L_d^e$	$B^f$	$\Gamma_b^g$	$\theta_v^h$	$\gamma_{e,\text{break}}^i$	$\gamma_{e,\text{max}}^l$	$s_1^m$	$s_2^n$
1H 0323+342	1.9 (650)	7.0	116	1.0	1.4 (0.9)	30	12	3	60	6000	-1	3.1
PKS 1502+036	24 (4000)	7.3	155	21	2.4 (0.8)	1.6	13	3	50	3000	1	3.2
PKS 2004-447	6 (4000)	6.7 <sup>o</sup>	39	3.1	0.15 (0.2)	6.9	8	3	120	1500	0.2	2
PMN J0948+0022*	72 (1600)	8.2	300	240	9 (0.4)	3.4	10	6	800	1600	1	2.2

<sup>a</sup>Dissipation radius in units of  $10^{15}$  cm and (in parenthesis) in units of the Schwarzschild radius.

<sup>b</sup>Black hole mass in units of  $M_\odot$  (details and caveats about the mass estimation used in this work can be found in Ghisellini et al. 2009a; the error with this method is generally about 50%).

<sup>c</sup>Size of the BLR in units of  $10^{15}$  cm.

<sup>d</sup>Power injected in the blob calculated in the comoving frame, in units of  $10^{41}$  erg s<sup>-1</sup>.

<sup>e</sup>Accretion disk luminosity in units of  $10^{45}$  erg s<sup>-1</sup> calculated by integrating the thermal component (black dotted line) of the SEDs in Fig. 1 and (in parenthesis) in Eddington units.

<sup>f</sup>Magnetic field in Gauss.

<sup>g</sup>Bulk Lorentz factor at  $R_{\text{diss}}$ .

<sup>h</sup>Viewing angle in degrees.

<sup>i</sup>Break random Lorentz factors of the injected electrons.

<sup>l</sup>Maximum random Lorentz factors of the injected electrons.

<sup>m</sup>Slope of the injected electron distribution below  $\gamma_{e,\text{break}}$ .

<sup>n</sup>Slope of the injected electron distribution above  $\gamma_{e,\text{break}}$ .

<sup>o</sup>Fixed from measurement with reverberation mapping method reported by Oshlack et al. (2001).

\*See Abdo et al. (2009a).

### 3. Spectral Energy Distributions (SED)

135

136 The SEDs built with all the available data are displayed in Fig. 1. As for PMN  
 137 J0948+0022, these SEDs show clear similarities with blazars and therefore we fitted them  
 138 with the synchrotron and inverse-Compton model developed by Ghisellini & Tavecchio

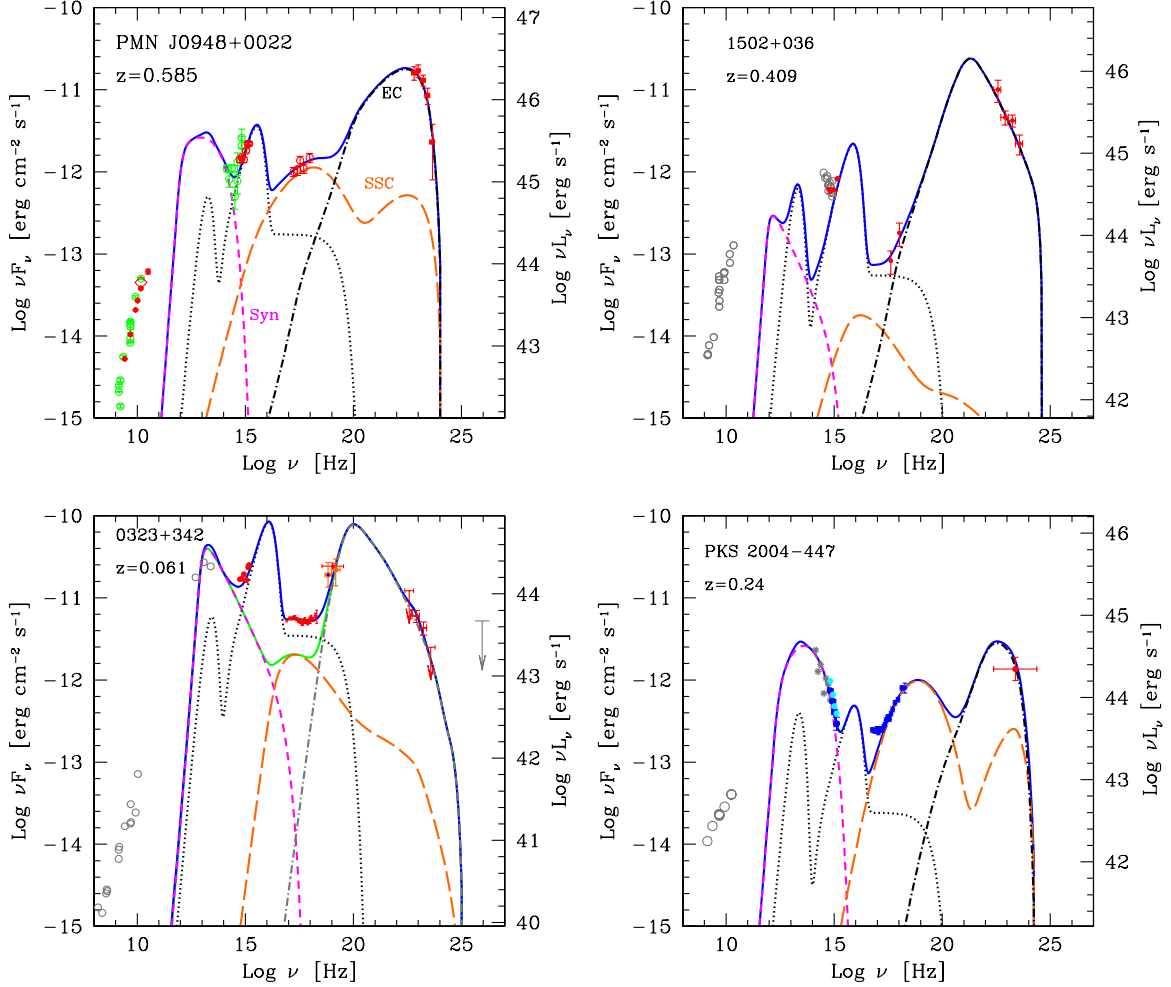


Fig. 1.— SEDs of the four RL-NLS1s detected by *Fermi*/LAT in order of decreasing  $\gamma$ -ray flux. The SED of PMN J0948+0022 is that from Abdo et al. (2009a). In the SED of 1H 0323+342, there are also detections in the hard X-rays by *Swift*/BAT (Cusumano et al. 2009) and *INTEGRAL*/ISGRI (Bird et al. 2007). The TeV upper limit is derived from observations with *Whipple* (Falcone et al. 2004). Archival radio data are from NED, but are displayed just for completeness, since they are not used in the model fit. The synchrotron self-absorption is clearly visible around  $10^{11-12}$  Hz. The short dashed light blue line indicates the synchrotron component, while the long dashed orange line is the SSC. The dot-dashed line refers to EC and the dotted black line represents the contribution of the accretion disk, X-ray corona and the IR torus. The continuous blue line is the sum of all the contributions.

Table 4: Power carried out by the jet.

Name	$\log P_r^a$	$\log P_B^b$	$\log P_e^c$	$\log P_p^d$
1H 0323+342	42.8	43.3	42.7	44.3
PKS 1502+036	44.0	43.0	44.1	46.2
PKS 2004+447	42.9	42.6	42.9	44.1
PMN J0948+0022*	45.3	44.3	44.7	46.7

<sup>a</sup>Radiative power [erg s<sup>-1</sup>].

<sup>b</sup>Poynting flux power [erg s<sup>-1</sup>].

<sup>c</sup>Power in bulk motion of electrons [erg s<sup>-1</sup>].

<sup>d</sup>Power in bulk motion of protons, assuming one proton per emitting electron [erg s<sup>-1</sup>].

\*See Abdo et al. (2009a).

140 law shape, of parameters  $\gamma_e^{-s_1}$  for energies below the break  $\gamma_{e,\text{break}}$  and  $\gamma_e^{-s_2}$  above, where  $\gamma_e$  is  
 141 the random Lorentz factor of electrons. This distribution is iteratively modified to take into  
 142 account electron cooling and the possibility to produce pairs through  $\gamma\gamma \rightarrow e^\pm$ . The resulting  
 143 distribution at the time  $R/c \approx 0.1R_{\text{diss}}/c$ , where  $R_{\text{diss}}$  is the dissipation radius and  $0.1R_{\text{diss}}$   
 144 is the size of the emitting spherical blob, is used to generate the radiation emitted through  
 145 the processes of synchrotron, synchrotron self-Compton (SSC) and external-Compton (EC).  
 146 The seed photons for the latter are the sum of several contributions: photons directly ra-  
 147 diated from the accretion disk (Dermer & Schlickeiser 1993), from the broad-line region  
 148 (BLR<sup>4</sup>, Sikora, Begelman & Rees 1994) and from the infrared torus (Błażejowski et al. 2000;  
 149 Sikora et al. 2002). We refer to Ghisellini & Tavecchio (2009) for more details. The model  
 150 parameters and the calculated powers are listed in Tables 3 and 4.

151 Archival radio data are displayed in Fig. 1 for completeness, but are not used in the  
 152 model fit. Indeed, the one-zone model used in the present work has to explain the bulk of the  
 153 emission and, therefore, necessarily requires a compact source. This, in turn, is self-absorbed  
 154 for synchrotron radiation (at  $\approx 10^{11-12}$  Hz). The radio emission is detectable only when the  
 155 blob becomes optically thin and this occurs as it moves and expands, further out in the jet  
 156 (e.g. Blandford & Königl, 1979).

157 Given the scarce, non-simultaneous data and the weakness of the  $\gamma$ -ray emission for  
 158 the three newly discovered sources, it is not possible to tightly constrain the selection of  
 159 parameters. As a guide to the selection of the initial values of the model parameters (Table 3),

---

<sup>4</sup>In the case of NLS1s, the permitted emission lines from the BLR are narrower than usual, with  $\text{FWHM}(\text{H}\beta) \lesssim 2000 \text{ km s}^{-1}$ .

160 we were driven by the recent (March-July 2009) multiwavelength study of PMN J0948+0022  
 161 (Abdo et al., 2009c), our knowledge of blazars, and the mass measurements performed with  
 162 other methods (particularly in the case of PKS 2004-447, for which the optical/UV data  
 163 are not sampling the accretion disk emission). When more information, particularly from  
 164 multiwavelength variability studies, will be available, it will be possible to improve the  
 165 estimation of the parameter values.

#### 166 4. Discussion

167 The analysis of the individual sources reveals some things worth noting. In 1H 0323+342  
 168 the dissipation region needs to be located very close to the central black hole ( $\sim 650$  times the  
 169 Schwarzschild radius  $R_S$ ) and hence a quite high magnetic field (up to 30 gauss) is needed. We  
 170 note that PKS 2004-447 seems to be different with respect to the three other RL-NLS1s, with  
 171 optical/UV data sampling the synchrotron emission instead of the accretion disk. Indeed, the  
 172 classification of this source is still open: while Oshlack et al. (2001) classified it as genuine  
 173 RL-NLS1, Komossa et al. (2006) suggested it can be a narrow-line radio galaxy, on the basis  
 174 that the bump of FeII is weak. Gallo et al. (2006) noted that there is no specific prescription  
 175 on the value of the strength of the FeII bump and confirmed the NLS1 classification. The  
 176 same authors noted that PKS 2004-447 is a compact steep-spectrum (CSS) radio source. On  
 177 the other hand, this source is also in the CRATES catalog of flat spectrum radio sources  
 178 (Healey et al. 2007), which includes also the three others NLS1s in this work. From the  
 179 present study, the estimated jet power of PKS 2004-447 is well above the range typical of  
 180 radio galaxies and, therefore, we favor the hypothesis of a genuine NLS1. However, in this  
 181 case the classification remains uncertain and should be studied with further observations.

182 A synoptic analysis of the 4 RL-NLS1s in the present work shows that PKS 1502+036  
 183 carries a jet power comparable to PMN J0948+0022, while the remaining two sources are  
 184 significantly less powerful – even two order of magnitudes for proton powers (Table 4). The  
 185 comparison with the large sample of blazars reported in Celotti & Ghisellini (2008) and  
 186 Ghisellini et al. (2009b), shows that the jet powers of PKS 1502+036 and PMN J0948+0022  
 187 are in the region of quasars, while 1H 0323+342 and PKS 2004-447 are in the range typical  
 188 of BL Lac Objects. The  $\gamma$ -ray emitting RL-NLS1s in our sample have small masses and  
 189 high accretion rates. This is in contradiction to the larger masses and smaller accretion  
 190 rates expected from low-power blazars (HFSRQs) with strong emission lines, as suggested  
 191 by Yuan et al. (2008). Anyway, when comparing the calculated powers with the distribution  
 192 of powers in blazars (quasars plus BL Lacs; see Ghisellini et al. 2009b), RL-NLS1s are in  
 193 the average range.

194 The main differences with respect to blazars are in the masses and accretion rates. The  
 195 masses of the three newly discovered RL-NLS1s are around  $10^7 M_\odot$ , in agreement within one  
 196 order of magnitude with the values obtained with other methods. In the case of 1H 0323+342,  
 197 Zhou et al. (2007) found values of  $1.8 \times 10^7 M_\odot$  with  $H\beta$  luminosity and  $3 \times 10^7 M_\odot$  with  
 198 the luminosity of the continuum at  $5100\text{\AA}$ . In the case of PKS 1502+036, Yuan et al. (2008)  
 199 estimate the mass to be  $4 \times 10^6 M_\odot$ , by means of the virial method. These value are about  
 200 1-2 orders of magnitude lower than the typical blazar masses ( $\approx 10^9 M_\odot$ , see Ghisellini et al.  
 201 2009b). The accretion rates can reach extreme values, up to 80 or even 90% the Eddington  
 202 values in the cases of PKS 1502+036 and 1H 0323+342, respectively. These values are the  
 203 most extreme ever found in any  $\gamma$ -ray emitting AGNs, but usual for NLS1s.

204 What is at odds with this scenario is the type of host galaxy, which is elliptical in all  
 205 blazars, while is likely to be spiral in RL-NLS1s (see, e.g. Zhou et al. 2006). In the case of  
 206 1H 0323+342, analysis of optical observations suggests two possibilities: Zhou et al. (2007)  
 207 show the spiral arms of the host galaxy by means of observations with the *Hubble Space*  
 208 *Telescope*, while Antòn et al. (2008), on the basis of ground-based observations with Nordic  
 209 Optical Telescope (NOT), suggest that these structures are the residual of a merging that  
 210 occurred within the past  $10^8$  years. This means that relativistic jets can form and develop  
 211 independently of their host galaxies, with quasars, BL Lacs and, now, RL-NLS1s jointly  
 212 characterized by the presence of a relativistic jet and with the differences in their observed  
 213 SEDs mainly determined by their masses and accretion rates.

214 The *Fermi* LAT Collaboration acknowledges generous ongoing support from a number  
 215 of agencies and institutes that have supported both the development and the operation of the  
 216 LAT as well as scientific data analysis. These include the National Aeronautics and Space  
 217 Administration and the Department of Energy in the United States, the Commissariat à  
 218 l’Energie Atomique and the Centre National de la Recherche Scientifique / Institut National  
 219 de Physique Nucléaire et de Physique des Particules in France, the Agenzia Spaziale Italiana  
 220 and the Istituto Nazionale di Fisica Nucleare in Italy, the Ministry of Education, Culture,  
 221 Sports, Science and Technology (MEXT), High Energy Accelerator Research Organization  
 222 (KEK) and Japan Aerospace Exploration Agency (JAXA) in Japan, and the K. A. Wallen-  
 223 berg Foundation, the Swedish Research Council and the Swedish National Space Board in  
 224 Sweden. Additional support for science analysis during the operations phase is gratefully  
 225 acknowledged from the Istituto Nazionale di Astrofisica in Italy and the Centre National  
 226 d’Études Spatiales in France.

227 This research has made use of the NASA/IPAC Extragalactic Database (NED) which  
 228 is operated by the Jet Propulsion Laboratory, California Institute of Technology, under  
 229 contract with the National Aeronautics and Space Administration and of data obtained

230 from the High Energy Astrophysics Science Archive Research Center (HEASARC), provided  
231 by NASA’s Goddard Space Flight Center.

## 232 REFERENCES

- 233 Abdo A.A., Ackermann M., Ajello M., et al., 2009a, ApJ, 699, 976
- 234 Abdo A.A., Ackermann M., Ajello M., et al., 2009b, ApJ, 700, 597
- 235 Abdo A.A., Ackermann M., Ajello M., et al., 2009c, ApJ, accepted for publication  
236 [arXiv:0910.4540]
- 237 Antòn S., Browne I.W.A., Marchã M.J., 2008, A&A, 490, 583
- 238 Atwood W.B., Abdo A.A., Ackermann M., et al., 2009, ApJ, 697, 1071
- 239 Bird A.J., Malizia A., Bazzano A., et al., 2007, ApJS, 170, 175
- 240 Blandford R.D. & Königl A., 1979, ApJ, 232, 34
- 241 Błażejowski M., Sikora M., Moderski R. & Madejski G.M., 2000, ApJ, 545, 107
- 242 Brunthaler A., Falcke H., Bower G.C., et al., 2000, A&A, 357, L45
- 243 Brunthaler A., Falcke H., Bower G.C., et al., 2005, A&A, 435, 497
- 244 Cardelli J.A., Clayton G.C., Mathis J.S., 1989, ApJ, 345, 245
- 245 Cash W., 1979, ApJ 228, 939
- 246 Celotti A. & Ghisellini G., 2008, MNRAS, 385, 283
- 247 Cusumano G., La Parola V., Segreto A., et al., 2009, A&A, accepted for publication  
248 [arXiv:0906.4788]
- 249 Dermer, C.D. & Schlickeiser, R., 1993, ApJ, 416, 458
- 250 Falcone A.D., Bond I.H., Boyle P.J., et al., 2004, ApJ, 613, 710
- 251 Foschini L., Ghisellini G., Raiteri C.M., et al., 2006, A&A, 453, 829
- 252 Foschini, L., et al., 2009a, in Proc. Conf. on ”Accretion and Ejection in AGN: a Global View”,  
253 ASP Conf. Proc., ed. L. Maraschi, G. Ghisellini, R. Della Ceca & F. Tavecchio (San  
254 Francisco, CA: ASP), in press (arXiv:0908.3313)

- 255 Foschini L., Maraschi L., Tavecchio F., Ghisellini G., Gliozzi M., Sambruna R.M., 2009b,  
256 *Adv. Space Res.*, 43, 889
- 257 Gallo L.C., Edwards P.G., Ferrero E., et al., 2006, *MNRAS*, 370, 245
- 258 Ghisellini G., Haardt F., Matt G., 2004, *A&A*, 413, 535
- 259 Ghisellini G. & Tavecchio F., 2009, *MNRAS*, 397, 985
- 260 Ghisellini G., Foschini L., Volonteri M., et al., 2009a, *MNRAS*, 399, L24
- 261 Ghisellini G., Tavecchio F., Foschini L., et al., 2009b, *MNRAS*, accepted for publication  
262 [[arXiv:0909.0932](https://arxiv.org/abs/0909.0932)]
- 263 Healey S.E., Romani R.W., Taylor G.B. et al., 2007, *ApJS*, 171, 61
- 264 Ho L.C., 2008, *ARA&A*, 46, 475
- 265 Kalberla P.M.W., Burton W.B., Hartmann D., et al., 2005, *A&A*, 440, 775
- 266 Leighly K.M., 1999, *ApJS*, 125, 317
- 267 Komatsu E., Dunkley J., Nolte M. R., et al., 2009, *ApJS*, 180, 330
- 268 Komossa S., Voges W., Xu D., et al., 2006, *ApJ*, 132, 531
- 269 Lister M.L., Aller H.D., Aller M.F., et al., 2009, *AJ*, 137, 3718
- 270 Maraschi L., Foschini L., Ghisellini G., et al., 2008, *MNRAS*, 391, 1981
- 271 Marscher A., 2009, In: “The Jet Paradigm - From Microquasars to Quasars”, edited by T.  
272 Belloni, *Lect. Notes Phys.* 794, in press [[arXiv:0909.2576](https://arxiv.org/abs/0909.2576)]
- 273 Mattox J.R., Bertsch D.L., Chiang J.L., et al., 1996, *ApJ*, 461, 396
- 274 Oshlack A.Y.K.N., Webster R.L., Whiting M.T., 2001, *ApJ*, 558, 578
- 275 Pogge R.W., 2000, *New Astronomy Reviews*, 44, 381
- 276 Rando R. et al., 2009, *Proceedings of the 31th ICRC*, [[arXiv:0907.0626](https://arxiv.org/abs/0907.0626)]
- 277 Sikora M., Begelman M.C. & Rees M.J., 1994, *ApJ*, 421, 153
- 278 Sikora M., Błażejowski M., Moderski R. & Madejski G.M., 2002, *ApJ*, 577, 78
- 279 Whalen D.J., Laurent-Muehleisen S.A., Moran E.C. & Becker R.H., 2006, *AJ*, 131, 1948

- <sup>280</sup> Yuan W., Zhou H.Y., Komossa S.A. et al., 2008, ApJ, 685, 801
- <sup>281</sup> Zhou H.-Y. & Wang T.-G., 2002, Ch. J. A&A, 2, 501
- <sup>282</sup> Zhou H.-Y., Wang T.-G., Yuan W.-M., et al., 2006, ApJS, 166, 128
- <sup>283</sup> Zhou H.-Y., Wang T.-G., Yuan W.-M., et al., 2007, ApJ, 658, L13